

1 Base-paired structure in the 5' untranslated region is required for the
2 efficient amplification of negative-strand RNA3 in the bromovirus
3 melandrium yellow fleck virus

4

5 Taiki Narabayashi, Masanori Kaido, Tetsuro Okuno, Kazuyuki Mise *

6

7 Laboratory of Plant Pathology, Graduate School of Agriculture, Kyoto University, Kyoto
8 606-8502, Japan

9

10 * Corresponding author at: Laboratory of Plant Pathology, Graduate School of Agriculture,
11 Kyoto University, Kitashirakawa, Sakyo-ku, Kyoto 606-8502, Japan. Tel: +81-75-753-6132;
12 Fax: +81 75 753 6131.

13 *E-mail address:* kmise@kais.kyoto-u.ac.jp (K. Mise).

14

1 **ABSTRACT**

2

3 *Melandrium yellow fleck virus* belongs to the genus *Bromovirus*, which is a group of tripartite
4 plant RNA viruses. This virus has an approximately 200-nucleotide direct repeat sequence in
5 the 5' untranslated region (UTR) of RNA3 that encodes the 3a movement protein. In the
6 present study, protoplast assays suggested that the duplicated region contains
7 amplification-enhancing elements. Deletion analyses of the 5' UTR of RNA3 showed that
8 mutations in the short base-paired region, which is located dozens of bases upstream of the
9 initiation codon of the 3a gene, greatly reduced the accumulation of RNA3. Disruption and
10 restoration of the base-paired structure caused the accumulation of RNA3 to be decreased and
11 restored, respectively. In vitro translation/replication assays demonstrated that the base-paired
12 structure is important for the efficient amplification of negative-strand RNA3. A similar
13 base-paired structure in RNA3 of another bromovirus, brome mosaic virus (BMV), also
14 facilitated the efficient amplification of BMV RNA3, but only in combination with
15 melandrium yellow fleck virus (MYFV) replicase and not with BMV replicase, thereby
16 suggesting specific interactions between base-paired structures and MYFV replicase.

17

18 *Keywords:* 5' untranslated region; *Bromovirus*; positive-strand RNA virus; protoplast; RNA
19 replication; RNA structure

20

1 **1. Introduction**

2

3 The genomic RNAs of all positive-strand RNA viruses have multifunctional roles. They
4 act as mRNAs to translate viral proteins and also as the templates for negative-strand RNA
5 synthesis. Thus, it is important to regulate these processes, and several RNA elements have
6 been identified that are required for these processes (Dreher, 1999; Liu et al., 2009; Noueir
7 and Ahlquist, 2003; Ogram and Flanagan, 2011; Pathak et al., 2011). Negative-strand RNA
8 synthesis is initiated near the 3' terminus, but the RNA elements required for negative-strand
9 RNA synthesis are located in the other regions of viral RNAs such as the 5' untranslated
10 region (UTR), as well as in the 3' UTR. The functions of these RNA elements have been
11 investigated, and they are known to be regulated by interactions between viral RNA elements,
12 or between viral RNA elements and proteins, including viral and host factors (Filomatori et
13 al., 2006; Herold and Andino, 2001; Noueir and Ahlquist, 2003; Pathak et al., 2011).

14 *Brome mosaic virus* is the type species of the genus *Bromovirus*, which is a group of
15 icosahedral plant RNA viruses in the family *Bromoviridae*. The genome comprises three
16 genomic RNAs, which are referred to as RNA1, RNA2, and RNA3 in order of their genome
17 sizes. RNA1 and RNA2 are monocistronic RNAs that encode the 1a and 2a proteins,
18 respectively, and both are required for genomic and subgenomic RNA4 synthesis (Kroner et
19 al., 1989; 1990). RNA3 is a dicistronic RNA that encodes the 3a protein required for
20 bromovirus movement (Mise et al., 1993) and the coat protein, which is translated from the
21 RNA4 that is transcribed from the negative-strand RNA3 (Miller et al., 1985).

22 The *cis*-acting RNA elements required for the negative-strand synthesis of brome mosaic
23 virus (BMV) genomic RNAs are well characterized. In the 3' UTR, the stem loop C within
24 the tRNA-like structure acts as the promoter for negative-strand synthesis (Kim et al., 2000).
25 The box B motif in the intercistronic region of RNA3 is recognized by the 1a protein, and

1 RNA3 is recruited to endoplasmic reticulum membrane invaginations where BMV replication
2 occurs (Schwartz et al., 2002; Sullivan and Ahlquist, 1999). The requirement for both the
3 intercistronic region and the 3' UTR of RNA3 for the formation of the replicase complex was
4 demonstrated in a yeast system (Quadt et al., 1995), which fully supports BMV replication
5 and transcription, as found in plant cells (Janda and Ahlquist, 1993). The 5' UTR of RNA2
6 also contains the box B motif, and it has been reported to be involved in translational
7 repression and RNA recruitment, which are key steps during negative-strand RNA synthesis
8 (Chen et al., 2001; Yi et al., 2007). However, although the 5' UTR of RNA3 was also shown
9 to be important for negative-strand RNA3 accumulation (Choi et al., 2004), the detailed roles
10 of the 5' UTR of RNA3 in negative-strand synthesis have remained unclear.

11 Previously, we constructed infectious cDNA clones for the bromovirus melandrium
12 yellow fleck virus (MYFV) and determined their nucleotide sequences, which showed that the
13 genomic RNA3 of MYFV has unique characteristics compared with those of other
14 bromoviruses (Narabayashi et al., 2009). Unlike BMV RNA3 having a poly(A) tract in the
15 intercistronic region between the 3a and coat protein genes, MYFV RNA3 lacks the poly(A)
16 tract, and it contains a duplicated sequence of about 200 bases with a short ORF around the
17 border of the duplicated regions in the 5' UTR. During cDNA cloning procedures, we also
18 found that 10% of the cDNA clones lacked the duplication in the 5' UTR of RNA3. These
19 minor clones had nucleotide sequences identical to those of the other major clones except for
20 the duplication. Co-infection experiments using RNA3 clones with or without the duplicated
21 sequence (3W and 3S, respectively, in Fig. 1A) demonstrated that the duplication contributed
22 to the competitive fitness of the virus in *Nicotiana benthamiana* plants (Narabayashi et al.,
23 2009). However, the functional role of this duplication in MYFV life cycles has not been
24 determined. In this study, we used both *N. benthamiana* protoplasts in vivo and an
25 evacuated BY-2 protoplast lysate (BYL) in vitro (Komoda et al., 2004) and identified a

1 novel RNA element within the duplicated region in the 5' UTR of MYFV RNA3, which is
2 required for the efficient amplification of MYFV RNA3, probably by enhancing
3 negative-strand amplification via specific interactions with its cognate replicase.

4

5 **2. Materials and methods**

6

7 *2.1. Plasmid construction*

8

9 The pMY3TP4 (3S) contains the same cDNA insert found in pMY3TP3 (3W), except it
10 lacks the duplicated region (Narabayashi et al., 2009). Before creating a series of plasmids
11 that encoded the C-terminal hemagglutinin (HA)-tagged 3a protein, we inserted three
12 nucleotides (GGC) that encoded a glycine spacer sequence and a HA-coding nucleotide
13 sequence (TACCCATACGATGTTCCAGATTACGCT) immediately upstream of the stop
14 codon of the 3a gene in pMY3TP4 (3S), thereby generating pMY3TP4-HA.

15 All of the primers used in this study are shown in Supplementary Table S1. The plasmids
16 with mutations in the 5' UTR of MYFV RNA3 were generated by PCR-mediated site-directed
17 mutagenesis of pMY3TP4-HA, which is a method referred to as “recombinant PCR” (Higuchi,
18 1990). The two pairs of primers used for primary PCR to amplify two DNA fragments were
19 M4 plus dn_R and dn_F plus MY3.13R-2 (n = 55–153, 104–202, 154–226, 154–252, 55–64,
20 65–81, 82–103, 203–217, and 218–229). The two resultant DNA fragments were recombined
21 by secondary PCR using M4 plus MY3.13R-2. The amplified DNA fragments were purified,
22 digested with *Hind*III and *Acc*I, and ligated into *Hind*III and *Acc*I-cut pMY3TP4-HA to
23 generate pMY3TP4-HA-dn (n = 55–153, 104–202, 154–226, 154–252, 55–64, 65–81, 82–103,
24 203–217, and 218–229). The following seven plasmids were constructed in a similar manner
25 using two or three pairs of appropriate primers for primary PCR. pMY3TP4-HA-rx (x = 1–1,

1 1–2, 2–1, and 2–2) was constructed using two pairs of primers: M4 plus rx_R and rx_F plus
2 MY3.13R-2 (x = 1–1, 1–2, 2–1, and 2–2). pMY3TP4-HA-dMB-1 was constructed using three
3 pairs of primers: M4 plus dMB-1_4, dMB-1_1 plus dMB-1_3, and dMB-1_2 plus
4 MY3.13R-2. pMY3TP4-HA-dMB-2 and pMY3TP4-HA-dMB-3 were constructed using two
5 pairs of primers: M4 plus dMB-2_2 and dMB-2_1 plus MY3.13R-2, or M4 plus dMB3_R and
6 dMB3_F plus MY3.13R-2, respectively.

7 To construct pBYL2MY1a and pBYLMY2a, cDNA fragments containing the 1a and 2a
8 genes were PCR-amplified from pMY1TP1 and pMY2TP2 (Narabayashi et al., 2009) using
9 two pairs of primers: pBYL-MY1a_F plus pBYL-MY1a_R and pBYL-MY2a_F plus
10 pBYL-MY2a_R (Supplementary Table S1), respectively. The amplified fragments were
11 digested with *AscI* and ligated into *AscI*-cut pBYL2 (Mine et al., 2010) in the correct
12 orientation.

13 BMV derivatives were generated by PCR-mediated site-directed mutagenesis of pB3TP8
14 (Janda et al., 1987) using the primer pairs Bd1_F plus Bd1_R and Bd2_F plus Bd2_R
15 (Supplementary Table S1). The amplified fragments were digested with *ClaI* and *SphI*, and
16 ligated into *ClaI* and *SphI*-cut pB3TP8 to generate pB3TP8-Bd1 and pB3TP8-Bd2,
17 respectively.

18

19 2.2. *In vitro* transcription and protoplast experiments

20

21 Transcripts of bromoviral RNAs were synthesized using T7 RNA polymerase (Takara,
22 Otsu, Japan) with the appropriate cap structure analog (m⁷GpppG; New England Biolabs,
23 Beverly, MA, USA), as described previously (Kroner and Ahlquist, 1992; Narabayashi et al.,
24 2009). mRNAs encoding MYFV 1a and 2a proteins were synthesized from *NotI*-linearized
25 pBYLMY1a and pBYLMY2a, respectively. All of the transcripts were purified using

1 Sephadex G-50 (GE Healthcare Bio-Sciences Corp., Piscataway, NJ, USA) gel
2 chromatography.

3 *N. benthamiana* protoplast assays were performed as described previously (Narabayashi
4 et al., 2009). Typically, $2\text{--}3 \times 10^5$ protoplasts were inoculated with 3.0 μg of transcripts (1 μg
5 each of RNA1, RNA2, and RNA3) and incubated for 20 h.

6 7 2.3. Northern blot analysis

8
9 Northern blot analysis of the total RNA was performed as described previously
10 (Narabayashi et al., 2009). To construct pMY3ES504 for detecting the negative strand of
11 MYFV RNA3, the 0.4-kb *SacI/EcoRV* fragments of pMY3TP3 were cloned into pBluescript
12 II (SK-) (Stratagene, La Jolla, CA). The negative-strand MYFV RNA3 was detected using
13 digoxigenin (DIG)-labeled T7 transcripts from *EcoRV*-linearized pMY3ES504. The
14 positive-strand BMV RNAs were detected using DIG-labeled riboprobes, which recognized
15 the 3' terminal region of all BMV RNAs (Kaido et al., 1995).

16 17 2.4. BYL experiments

18
19 The preparation of BYL and the in vitro translation/replication reaction were performed
20 as described previously (Iwakawa et al., 2007; Komoda et al., 2004). The mRNAs encoding
21 1a and 2a proteins, which were transcribed from pBYL2-MY1a and pBYL-MY2a,
22 respectively, were incubated in BYL at 25 °C for 2 h. Aliquots (24 μl) of the reaction mixture
23 were incubated further with bromovirus RNA3 and its derivatives at 25 °C for 2 h. The total
24 RNAs were then extracted and used for the Northern blot analysis.

25 For RNA stability assay, 0.5 μg of capped transcripts were incubated at 25 °C in 40 μl of

1 BYL reaction mixture. At 0, 0.5, 1 and 2 h after incubation, aliquots (10 μ l) were used for
2 RNA extraction, and subjected to Northern blot analysis.

3

4 **3. Results**

5

6 *3.1. The 3W levels were higher than the 3S levels in a competition assay using N.*
7 *benthamiana protoplasts*

8

9 We assumed that the differences in competitive fitness between 3W and 3S in whole *N.*
10 *benthamiana* plants (Narabayashi et al., 2009) might reflect the replication efficiency at the
11 single-cell levels. To verify this assumption, we inoculated *N. benthamiana* protoplasts with
12 an equimolar mixture of 3W and 3S, and RNAs 1 and 2 of MYFV. The Northern blot analysis
13 showed that the levels of RNA3 were similar after individual infection with 3W or 3S,
14 whereas 3W accumulated to 30% higher than 3S following coinfection (Figs. 1B and 1C).
15 This suggests that there is competition for replication between 3W and 3S, and that the
16 competitive fitness is determined at least partly during the replication step. Given that both of
17 the 5' and 3' terminal regions, as well as intercistronic regions, are required for the efficient
18 amplification of BMV RNA3s (French and Ahlquist, 1987), this duplicated region in the
19 internal site of the 5' UTR of MYFV RNA3 might contain previously undefined element(s)
20 that enhance the efficient amplification of bromoviral RNA3.

21

22

23 *3.2. Regions in the 5' UTR required for efficient amplification of RNA3*

24

25 To identify the putative *cis*-acting replication elements in the duplicated region (nt 55–

1 252), we constructed RNA3 derivatives that contained a series of 100-base deletions in the 5'
2 UTR and the 5' proximal sequences of the 3a-ORF (d55–153, d104–202, and d154–252; Fig.
3 2A). To exclude the possibility that the effects of the deletion of one element in the duplicated
4 region (light gray region in Fig. 1A) on RNA3 accumulation may have been masked or
5 attenuated by another element because of the duplication in 3W, we introduced deletions into
6 the 5' UTR of 3S (dark gray region in Fig. 1A) but not into that of 3W. The resultant RNA3
7 derivatives, and RNA1 and RNA2, were inoculated into *N. benthamiana* protoplasts, and the
8 accumulation of MYFV RNAs was analyzed by Northern blotting. The d55–153 and d154–
9 252 mutations, but not the d104–202 mutation, reduced the accumulation of RNA3 and
10 RNA4 in protoplasts (Fig. 2B). These results suggest that the two regions, i.e., one from nt
11 55–103 and the other from nt 203–252, contain nucleotide sequences and/or structures that
12 play important roles in the accumulation of RNA3 and RNA4.

13 The d154–252 mutant lacked a partial 5' coding sequence from the 3a gene, so we
14 examined whether this short coding region had any functions during RNA3 accumulation. A
15 d154–226 mutant was constructed with a deletion in the same region as d154–252 apart from
16 the 5' coding region of the 3a gene, which was tested in *N. benthaminana* protoplasts. The
17 accumulation of RNA3 and RNA4 from d154–226 was comparable to that of RNA3 and
18 RNA4 from d154–252 (Fig. 2B), thereby suggesting that deletions in the 5' UTR of MYFV
19 RNA3 but not the 3a-coding region reduced the accumulation of RNA3 and RNA4
20 dramatically. Subsequently, we focused on the functions of the 5' UTR of MYFV RNA3
21 during RNA3 accumulation.

22 To characterize further the RNA elements involved in RNA3 accumulation, we predicted
23 the secondary RNA structures in the 5' UTR of RNA3 using M-fold version 3.2 (Zuker, 2003),
24 which showed that the two regions (one from nt 55–103 and the other from nt 203–252)
25 formed a long base-paired structure with each other (Fig. 3A). To delimit the regions that

1 could affect the accumulation of RNA3, we constructed five mutants with deletions covering
2 the two regions in the 5' UTR of RNA3 (d55–64, d65–81, d82–103, d203–217, and d218–
3 229; Fig. 3B), and we examined their accumulation in *N. benthamiana* protoplasts when they
4 were inoculated together with MYFV RNA1 and RNA2 transcripts. Three deletions (nt 55–64,
5 nt 65–81, and nt 218–229) did not affect the accumulation of RNA3 or RNA4, whereas two
6 deletions (nt 82–103 and nt 203–217) reduced the levels of RNA3 and RNA4 greatly (Fig.
7 3C). These two sequences were predicted to form a base-paired structure with each other,
8 which was divided into two stems by an internal loop, thereby suggesting that either or both
9 stems were important for the accumulation of RNA3 and RNA4.

10 To identify the functional domain and to determine the importance of the base-paired
11 structure for the accumulation of RNA3, we introduced nucleotide substitutions into either or
12 both sides of the two stems in this region, which disrupted or restored the base-pairing of the
13 stems, respectively (Fig. 4A). Disruption of the upper stem structure on either side of this
14 region by nucleotide substitutions (r1–1, r1–2) severely decreased the accumulation of RNA3
15 and RNA4, whereas the restoration of the stem (r1–3) restored the RNA3 and RNA4 levels to
16 that of 3S in *N. benthamiana* protoplasts (Figs. 4B and 4C). Furthermore, these mutations also
17 affected the accumulation of negative-strand RNA3 in parallel with that of positive-strand
18 RNA3 (Figs. 4B and 4C). In contrast to the upper stem, the mutations in the lower stem (r2–1,
19 r2–2, r2–3) did not affect the accumulation of positive- or negative-strand RNA3 (Fig. 4B).
20 Overall, these results suggest that the upper stem structure plays a crucial role in the in vivo
21 accumulation of positive- and negative-strand RNA3.

22

23 *3.3. The base-paired structure is involved in the efficient amplification of negative-strand*
24 *RNA3*

25

1 The mutations in the base-paired structure reduced the in vivo accumulation of
2 negative-strand RNA3 (Fig. 4), but it was still unclear whether this reduction was caused by
3 decreases in negative- and/or positive-strand RNA3 synthesis. To determine whether this
4 base-paired structure has a role in the amplification of negative-strand RNA3, we performed
5 an in vitro translation/replication BYL assay (Komoda et al., 2004). RNA3 derivatives were
6 incubated in BYL that expressed the 1a and 2a proteins of MYFV, and the positive- and
7 negative-strand RNA accumulation levels were examined. Similar to the in vivo results (Fig.
8 4), the accumulation of negative-strand RNA3 in BYL was again reduced significantly by the
9 disruption mutations (r1-1, r1-2) and recovered by the restoration mutation (r1-3) (Fig. 5).
10 However, the levels of positive-strand RNA3 in BYL were not changed significantly by either
11 the disruption (r1-1, r1-2) or restoration (r1-3) of the structure in either the presence or
12 absence of the 1a and 2a proteins of MYFV (Fig. 5A, Supplementary Figure S2, data not
13 shown). Together, these results mainly reflected the stability of the input transcripts rather
14 than the levels of newly synthesized positive-strand RNA3, as discussed below. These in vitro
15 results suggest that the reduction in negative-strand accumulation in protoplasts was
16 attributable at least partly to a reduction in the efficient amplification of negative-strand
17 RNA3 but not necessarily to the indirect effect of the inefficient amplification of
18 positive-strand RNA3. These results also suggest that this base-paired region (nt 89–95 and nt
19 203–209) in the 5' UTR of RNA3 is involved in the efficient amplification of negative-strand
20 RNA3, thereby affecting the accumulation of both negative- and positive-strand RNA3s and
21 subgenomic RNA4 in protoplasts (Fig. 4B).

22

23 *3.4. Comparison between MYFV and other bromoviruses*

24

25 Next, we investigated whether the base-paired structure of the 5' UTR of RNA3 was also

1 seen in other bromoviruses. In the 5' UTRs of bromoviruses, base-paired structures that
2 comprised 7–8 base pairs containing the initiation codon (AUG) of 3a-ORF were predicted
3 using the M-fold program (Fig. 6A). The base-paired structure of MYFV did not contain the
4 AUG sequence, but the four consecutive base pairs (5'-UCGG-3')/(5'-CCGA-3') were
5 conserved among MYFV, BMV, and cowpea chlorotic mottle virus (CCMV) (Fig. 6A). In
6 addition, the results shown in Fig. 4 demonstrate the importance of the structure rather than
7 the sequence for the efficient amplification of MYFV RNA3. Thus, we hypothesize that these
8 base-paired structures may have functions during the efficient amplification of bromoviral
9 RNA3.

10 To test whether a similar base-paired structure in RNA3 of another bromovirus, BMV,
11 functions during the amplification of MYFV RNA3, we introduced mutations into the 5' UTR
12 of MYFV RNA3. The d-MB1 mutation deleted most of the base-paired structure, except for
13 three G-C pairs (nt 65–92 and nt 206–229 deletions). The d-MB2 mutation was a four-base
14 insertion into d-MB1, which formed a base-paired structure similar to that in BMV. The
15 d-MB3 mutation replaced the base-paired region of MYFV with the corresponding region of
16 the BMV sequence (Fig. 6B). These mutants were tested to determine their accumulation
17 levels in *N. benthamiana* protoplasts, which were inoculated together with MYFV RNA1 and
18 RNA2 transcripts, as described above. Northern blot analysis showed that RNA3
19 accumulation was eliminated by the d-MB1 mutation, whereas it was restored by the d-MB2
20 and d-MB3 mutations (Fig. 6C). These results suggest that the base-paired structure of MYFV
21 RNA3 can be replaced with the corresponding structure of BMV RNA3, thereby confirming
22 the importance of the structure rather than the sequence.

23 To determine whether the base-paired structure of BMV RNA3 is involved in the
24 efficient amplification of the parental genome, two deletion mutations were introduced into
25 the 5' UTR of BMV RNA3 (Bd1: nt 79–91 and Bd2: nt 53–91), which resulted in disruptions

1 of the base-paired structure of BMV (Fig. 6D). When these mutants were inoculated together
2 with BMV RNA1 and RNA2 into *N. benthamiana* protoplasts, the deletions slightly reduced
3 RNA3 accumulation and increased RNA4 accumulation (Fig. 6E). BMV RNA3 could be
4 replicated after inoculation with MYFV RNA1 and RNA2 (Fig. 6E), so we also examined the
5 accumulation of Bd1 and Bd2 in the presence of MYFV RNA1 and RNA2. The deletions
6 eliminated the accumulation of RNA3 and RNA4 (Fig. 6E). Thus, the base-paired structure of
7 BMV RNA3 was essential for the efficient amplification of RNA3 by MYFV replicase,
8 whereas this structure was not crucial for RNA3 amplification by BMV replicase. These
9 results suggest that the function of the base-paired structure is correlated with the properties
10 of the MYFV replicase.

11

12 **4. Discussion**

13

14 In the present study, we analyzed RNA elements in the 5' UTR of bromoviral RNA3 that
15 enhance RNA3 amplification. The function of the RNA element required for the efficient
16 amplification of the negative-strand RNA3 of MYFV was shown to be sequence independent
17 but structure dependent, and it was identified as the base-paired structure in the 5' UTR of
18 MYFV RNA3, analogues of which were also found in other bromoviral RNA3s. Our analysis
19 of the effects of structural elements in BMV RNA3 demonstrated that the requirement for
20 base-paired structures for RNA3 amplification differed among distinct bromoviral replicases.

21 The 5' UTR of positive-strand RNA genomes corresponds to the 3' UTR of the negative
22 strand, which contains a promoter for positive-strand RNA synthesis. Thus, mutations in the
23 5' UTR could affect positive-strand RNA synthesis. In BMV, mutations in the 5' UTR of
24 RNA3, which affected the promoter activity of positive-strand RNA3 synthesis, had only
25 modest effects on negative-strand RNA3 accumulation, despite the low accumulation of

1 positive-strand RNA3s (Hema and Kao, 2004). Moreover, several mutations that substantially
2 decreased positive-strand RNA3 accumulation increased subgenomic RNA4 accumulation
3 (Grdzelishvili et al., 2005; Hema and Kao, 2004). These viral RNA accumulation patterns
4 were also observed in our deletion analysis of the base-paired structure of BMV RNA3 when
5 it was inoculated with BMV RNAs 1 and 2 (Fig. 6E). Thus, if the base-paired structure of the
6 5' UTR of bromoviral RNA3 functions during positive-strand synthesis but not during
7 negative-strand synthesis, mutations in this structure should change the levels of
8 positive-strand RNA3 relative to that of subgenomic RNA4 but would have only mild effects
9 on negative-strand accumulation. However, disruptions of the base-paired structures of the 5'
10 UTR of RNA3s dramatically reduced the accumulation of negative- and positive-strand
11 RNA3 and subgenomic RNA4 in vivo (Figs. 4, 6C, and 6E). Therefore, although we cannot
12 exclude the possibility that the base-paired structures may play an additional role in
13 positive-strand RNA3 synthesis by MYFV replicase, similar to that by BMV replicase, the
14 results of the protoplast assays strongly suggest that the base-paired structure functions
15 mainly during the efficient amplification of negative-strand RNA3.

16 In the in vitro BYL assays, the accumulation of positive-strand RNA3 was
17 indistinguishable among 3S and its derivatives (Fig. 5), which did not correlate with that of
18 negative-strand RNA3. Capped transcripts are stable in BYL, and large portions of input
19 transcripts could be detected even after incubation for several hours (Supplementary Figure
20 S2; Sarawaneeyaruk et al., 2009). Moreover, RNA4 accumulation was never observed (data
21 not shown), suggesting that positive-strand RNA synthesis from negative-strand RNA3 was
22 negligible. Therefore, most, if not all, of the positive-stranded RNA3s detected reflected input
23 transcripts, which indicated that the low accumulation of negative-strand RNA3 in vitro was
24 not a major consequence of the indirect effects of low positive-strand RNA3 synthesis. These
25 in vitro results support the in vivo results obtained with protoplasts, and they also indicate that

1 the base-paired region in the 5' UTR of MYFV RNA3 is involved in the efficient
2 amplification of negative-strand RNA3. Efficient amplification of negative-strand RNA3
3 results from efficient synthesis and/or high stability of negative-strand RNA3. If stable
4 double-stranded RNA but not free/naked negative-strand RNA would be generated as a result
5 of negative strand synthesis during MYFV replication like tombusvirus replication (Kovalev
6 et al., 2014), the base-paired structure in the 5'UTR may function in synthesizing negative
7 strand RNA3 rather than conferring stability on the nascent negative-strand RNA3.

8 The 5' UTR of BMV RNA3 is not required for the formation of the RNA-dependent
9 RNA polymerase complex (Quadt et al., 1995) or for replicase binding (Choi et al., 2004).
10 Our results also show that the base-paired structure of BMV RNA3 exerts only modest effects
11 on RNA amplification directed by BMV replicase compared with that directed by MYFV
12 replicase (Fig. 6E). In the bromovirus CCMV, deletions of the regions containing the
13 base-paired structure that corresponded to that of MYFV (Fig. 6A) had little effect on RNA3
14 accumulation, whereas deletions of another region of the 5' UTR suppressed the accumulation
15 of RNA3 and RNA4 (Pacha et al., 1990). Thus, although the 5' UTR of bromovirus RNA3s
16 might have general effects on the amplification of the negative-strand RNA3s of
17 bromoviruses, it is not known whether the base-paired structures of BMV and CCMV RNA3s
18 play roles during RNA3 replication by their own replicases. However, the base-paired
19 structure of BMV was shown to function during the efficient amplification of RNA3 (Fig. 6),
20 possibly by enhancing the amplification of negative-strand RNA3 in the presence of the
21 heterologous replicase of MYFV. This variable requirement for the base-paired structure by
22 distinct bromoviral replicases (Fig. 6E) suggests that in contrast to BMV, the base-paired
23 structure in the 5' UTR of RNA3 may be required for replicase assembly in MYFV.

24 In positive-strand RNA viruses, the transition from the translation to the replication of
25 genomic RNAs is a key step during the RNA replication cycle because template competition

1 occurs between these two processes (Gamarnik and Andino, 1998). The *cis*-acting elements
2 required for negative-strand synthesis have been found in the 5' UTR of their genomic RNAs,
3 and they are thought to regulate the transition through RNA–RNA interactions or RNA–
4 protein interactions (Filomatori et al., 2006; Herold and Andino, 2001). In BMV, the
5 repression of RNA1 and RNA2 translation is regulated by the interaction between the
6 replicase protein 1a and the box B motif in their 5' UTR, which may be related to replicase
7 assembly (Chen et al., 2001; Yi et al., 2007), whereas the RNA3s of four bromoviruses
8 including BMV and MYFV contain the box B motif in the intercistronic region. In two other
9 bromoviruses, CCMV and broad bean mottle virus, the RNA3s do not even contain the box B
10 motif (Allison et al., 1989; Romero et al., 1992). Thus, although some host factors have been
11 reported to be involved in the translation and recruitment of BMV RNA3 (Diez et al., 2000;
12 Mas et al., 2006), the detailed mechanisms that regulate translational repression and the
13 transition from translation to replication in RNA3 are still unclear. In the present study, we
14 identified a novel RNA element of MYFV RNA3, which is required for the efficient
15 amplification of negative-strand in the 5' UTR of RNA3, and we found that its function is
16 MYFV replicase specific. These findings will facilitate the development of a better
17 understanding of the life cycle of bromovirus RNA3.

18

19 **Acknowledgments**

20

21 This work was supported in part by a Grant-in-Aid for Scientific Research on Innovative
22 Areas (24120006) from the Japanese Ministry of Education, Culture, Sports, Science and
23 Technology, and a Grant-in-Aid for Scientific Research (B) (22380030) and a Grant-in-Aid
24 for Scientific Research (A) (22248002) from the Japan Society for the Promotion of Science
25 (JSPS). T.N. was a JSPS research fellow.

1
2
3
4
5
6
7
8
9
10
11
12
13
14
15
16
17
18
19
20
21
22
23
24
25

References

- Allison, R.F., Janda, M., Ahlquist, P., 1989. Sequence of cowpea chlorotic mottle virus RNAs 2 and 3 and evidence of a recombination event during bromovirus evolution. *Virology* 172, 321–330.
- Chen, J., Noueir, A., Ahlquist, P. 2001. Brome mosaic virus protein 1a recruits viral RNA2 to RNA replication through a 5' proximal RNA2 signal. *J. Virol.* 75, 3207–19.
- Choi, S.K., Hema, M., Gopinath, K., Santos, J., Kao, C., 2004. Replicase-binding sites on plus- and minus-strand brome mosaic virus RNAs and their roles in RNA replication in plant cells. *J. Virol.* 78, 13420–13429.
- Diez, J., Ishikawa, M., Kaido, M., Ahlquist, P., 2000. Identification and characterization of a host protein required for efficient template selection in viral RNA replication. *Proc. Natl. Acad. Sci. U.S.A.* 97, 3913–3918.
- Dreher, T.W., 1999. Functions of the 3'-untranslated regions of positive strand RNA viral genomes. *Annu. Rev. Phytopathol.* 37, 151–174.
- Filomatori, C.V., Lodeiro, M.F., Alvarez, D.E., Samsa, M.M., Pietrasanta, L., Gamarnik, A.V., 2006. A 5' RNA element promotes dengue virus RNA synthesis on a circular genome. *Gen. Dev.* 20, 2238–2249.
- French, R., Ahlquist, P., 1987. Intercistronic as well as terminal sequences are required for efficient amplification of brome mosaic virus RNA3. *J. Virol.* 61, 1457–1465.
- Gamarnik, A.V., and Andino, R., 1998. Switch from translation to RNA replication in a positive-stranded RNA virus. *Genes Dev.* 12, 2293–2304.
- Grdzlishvili, V.Z., Garcia-Ruiz, H., Watanabe, T., Ahlquist, P., 2005. Mutual interference between genomic RNA replication and subgenomic mRNA transcription in brome

- 1 mosaic virus. *J. Virol.* 79, 1438–1451.
- 2 Hema, M., Kao, C.C., 2004. Template sequence near the initiation nucleotide can modulate
3 brome mosaic virus RNA accumulation in plant protoplasts. *J. Virol.* 78, 1169–1180.
- 4 Herold, J., Andino, R., 2001. Poliovirus RNA replication requires genome circularization
5 through a protein-protein bridge. *Mol. Cell* 7, 581–591.
- 6 Higuchi, R., 1990. Recombinant PCR. in: Innis, M.A., Gelfand, D.H., Sninsky, J.J., and
7 White, T.J. (Eds.), *PCR Protocols*. Academic Press, San Diego, pp. 177–183.
- 8 Iwakawa, H-O., Kaido, M., Mise, K., Okuno, T., 2007. *cis*-Acting core RNA elements
9 required for negative-strand RNA synthesis and cap-independent translation are
10 separated in the 3'-untranslated region of *Red clover necrotic mosaic virus* RNA1.
11 *Virology* 369, 168–181.
- 12 Janda, M., French, R., Ahlquist, P., 1987. High efficiency T7 polymerase synthesis of
13 infectious RNA from cloned brome mosaic virus cDNA and effects of 5' extensions on
14 transcript infectivity. *Virology* 158, 259–262.
- 15 Janda, M., Ahlquist, P., 1993. RNA-dependent replication, transcription, and persistence of
16 brome mosaic virus RNA replicons in *S. cerevisiae*. *Cell* 72, 961–970.
- 17 Kaido, M., Mori, M., Mise, K., Okuno, T., Furusawa, I., 1995. Inhibition of brome mosaic
18 virus (BMV) amplification in protoplasts from transgenic tobacco plants expressing
19 replicable BMV RNAs. *J. Gen. Virol.* 76, 2827–2833.
- 20 Kim, C.H., Kao, C.C., Tinoco, I.Jr. 2000. RNA motifs that determine specificity between a
21 viral replicase and its promoter. *Nat. Struct. Biol.* 7, 415–423.
- 22 Komoda, K., Naito, S., Ishikawa, M., 2004. Replication of plant RNA virus genomes in a
23 cell-free extract of evacuated plant protoplasts. *Proc. Natl. Acad. Sci. U.S.A.* 101,
24 1863–1867.
- 25 Kovalev, N., Pogany, J., Nagy, P.D., 2014. A template role of double-stranded RNA in

- 1 tombusvirus replication. *J. Virol.* 88, (in press). doi:10.1128/JVI.03842-13.
- 2 Kroner, P., Ahlquist, P., 1992. RNA-based viruses. in: Gurr S.J., McPherson M.J., Bowles
3 D.J. (Eds.), *Molecular Plant Pathology; a Practical Approach*, Vol 1. Oxford University
4 Press, New York, pp. 23–34.
- 5 Kroner, P.A., Young, B.M., Ahlquist, P., 1990. Analysis of the role of brome mosaic virus 1a
6 protein domains in RNA replication, using linker insertion mutagenesis. *J. Virol.* 64,
7 6110–6120.
- 8 Kroner, P., Richards, D., Traynor, P., Ahlquist, P., 1989. Defined mutations in a small region
9 of the brome mosaic virus 2 gene cause diverse temperature-sensitive RNA replication
10 phenotypes. *J. Virol.* 63, 5302–5309.
- 11 Liu Y, Wimmer E, Paul AV. 2009. Cis-acting RNA elements in human and animal
12 plus-strand RNA viruses. *Biochim. Biophys. Acta.* 1789, 495–517.
- 13 Mas, A., Alves-Rodrigues, I., Noueir, A., Ahlquist, P., Diez, J. 2006. Host
14 deadenylation-dependent mRNA decapping factors are required for a key step in brome
15 mosaic virus RNA replication. *J. Virol.* 80, 246–251.
- 16 Miller, W.A., Dreher, T.W., Hall, T.C. 1985. Synthesis of brome mosaic virus subgenomic
17 RNA in vitro by internal initiation on (-)-sense genomic RNA. *Nature* 313, 68–70.
- 18 Mine, A., Takeda, A., Taniguchi, T., Taniguchi, H., Kaido, M., Mise, K., Okuno, T., 2010.
19 Identification and characterization of the 480-kilodalton template-specific RNA
20 dependent RNA polymerase complex of *Red clover necrotic mosaic virus*. *J. Virol.* 84,
21 6070–6081.
- 22 Mise, K., Allison, R.F., Janda, M., and Ahlquist, P., 1993. Bromovirus movement protein
23 genes play a crucial role in host specificity. *J. Virol.* 67, 2815–2823.
- 24 Narabayashi, T., Iwahashi, F., Kaido, M., Okuno, T., Mise, K., 2009. *Melandrium yellow*
25 *fleck bromovirus* infects *Arabidopsis thaliana* and has genomic RNA sequence

- 1 characteristics that are unique among bromoviruses. *Arch. Virol.* 154, 1381–1389.
- 2 Noueiry, A.O., Ahlquist, P., 2003. Brome mosaic virus RNA replication: revealing the role of
3 the host in RNA virus replication. *Annu. Rev. Phytopathol.* 41, 77–98.
- 4 Ogram, S.A., Flanagan, J.B., 2011. Non-template functions of viral RNA in picornavirus
5 replication. *Curr. Opin. Virol.* 1, 339–346.
- 6 Pacha, R.F., Allison, R.F., Ahlquist, P., 1990. *cis*-Acting sequences required for in vivo
7 amplification of genomic RNA3 are organized differently in related bromoviruses.
8 *Virology* 174, 436–443.
- 9 Pathak, K.B., Pogany, J., Nagy, P.D., 2011. Non-template functions of the viral RNA in plant
10 RNA virus replication. *Curr. Opin. Virol.* 1, 332–338.
- 11 Quadt, R., Ishikawa, M., Janda, M., Ahlquist, P., 1995. Formation of brome mosaic virus
12 RNA-dependent RNA polymerase in yeast requires coexpression of viral proteins and
13 viral RNA. *Proc. Natl. Acad. Sci. U.S.A.* 92, 4892–4896.
- 14 Romero, J., Dzianott, A.M., Bujarski, J.J., 1992. The nucleotide sequence and genome
15 organization of the RNA2 and RNA3 segments in broad bean mottle virus. *Virology* 187,
16 671–681.
- 17 Sarawaneeyaruk, S., Iwakawa, H.O., Mizumoto, H., Murakami, H., Kaido, M., Mise, K.,
18 Okuno, T., 2009. Host-dependent roles of the viral 5' untranslated region (UTR) in RNA
19 stabilization and cap-independent translational enhancement mediated by the 3' UTR of
20 *Red clover necrotic mosaic virus* RNA1. *Virology* 391, 107–118.
- 21 Schwartz, M., Chen, J., Janda, M., Sullivan, M., den Boon, J., Ahlquist, P., 2002. A
22 positive-strand RNA virus replication complex parallels form and function of retrovirus
23 capsids. *Mol. Cell* 9, 505–514.
- 24 Sullivan, M.L., Ahlquist, P., 1999. A brome mosaic virus intergenic RNA3 replication signal
25 functions with viral replication protein 1a to dramatically stabilize RNA in vivo. *J. Virol.*

1 73, 2622–2632.

2 Yi, G., Gopinath, K., Kao, C.C., 2007. Selective repression of translation by the brome
3 mosaic virus 1a RNA replication protein. *J. Virol.* 81, 1601–1609.

4 Zuker, M., 2003. Mfold web server for nucleic acid folding and hybridization
5 prediction. *Nucleic Acids Res.* 31, 3406–3415.

6

1 **Figure captions**

2

3 **Fig. 1.** Competition between 3W and 3S in *Nicotiana benthamiana* protoplasts. (A)
4 Schematic representation of the 5' UTR of 3W and 3S. The open bar indicates the 5' terminal
5 region that is not duplicated. The light-gray region represents the duplicate region of the
6 dark-gray region in the 5' UTR of melandrium yellow fleck virus (MYFV) RNA3. Schematic
7 representations of the predicted structures are also shown. Supplementary Fig. S1 shows the
8 predicted structures based on nucleotide sequences. (B) Northern blot analysis of viral RNA
9 accumulation in *N. benthamiana* protoplasts inoculated with a mixture of equimolar amounts
10 of 3W and 3S, and MYFV RNA1 and RNA2. Ethidium bromide-stained rRNA is shown as a
11 loading control. (C) The histogram represents the accumulation ratios of 3W compared with
12 3S during competition. The levels were measured using the ImageJ program, and the mean
13 value and the standard deviation were calculated based on six independent experiments.

14

15 **Fig. 2.** Deletion analysis of the 5' UTR of melandrium yellow fleck virus (MYFV) RNA3.
16 (A) Schematic representation of the deleted regions in the 5' UTR of 3S. Nucleotide deletions
17 are indicated by bent lines where the nucleotide numbers are shown at their 5' and 3' ends. (B)
18 Northern blot analysis of viral RNA accumulation in *Nicotiana benthamiana* protoplasts
19 inoculated with 3S or its variants, together with MYFV RNA1 and RNA2.

20

21 **Fig. 3.** Structure-based deletion analysis of the 5' UTR of melandrium yellow fleck virus
22 (MYFV) RNA3. (A) Schematic representations of the predicted secondary structures of the
23 regions, including the *cis*-element involved in 3S amplification. (B) Schematic
24 representations of the deleted regions in the 5' UTR of 3S. Nucleotide deletions are indicated
25 by bent lines where the nucleotide numbers are shown at their 5' and 3' ends. (C) Northern

1 blot analysis of viral RNA accumulation in *Nicotiana benthamiana* protoplasts inoculated
2 with 3S or its variants, together with MYFV RNA1 and RNA2.

3
4 **Fig. 4.** Analysis of the *cis*-acting RNA elements required for the efficient amplification of
5 melandrium yellow fleck virus (MYFV) RNA in vivo. (A) Schematic representation of the
6 secondary structure of the base-paired region. The disrupted and restored helical regions are
7 shown. Substituted nucleotides are indicated by boldface italic fonts. (B) Northern blot
8 analysis of positive (+)- and negative (-)-strand RNA accumulation in *Nicotiana benthamiana*
9 protoplasts inoculated with 3S or its variants, together with MYFV RNA1 and RNA2. (C)
10 Relative accumulation of positive- or negative-strand RNA3 by upper stem mutants compared
11 with that using 3S. The histogram compares the levels of the positive strand (dark-gray bars)
12 or negative strand (light-gray bars) of the tested RNA3 derivatives with that of the positive or
13 negative strand of 3S, respectively. The levels were measured using the ImageJ program, and
14 the mean value and the standard deviation were calculated based on three independent
15 experiments.

16
17 **Fig. 5.** In vitro RNA replication assay of the upper stem mutants of melandrium yellow fleck
18 virus (MYFV) RNA3. (A) Accumulation of positive- and negative-strand RNA3 in
19 evacuated BY-2 protoplast lysates incubated for 2 h with mRNA that expressed MYFV 1a
20 and 2a proteins, followed by 2 h with 3S or its variants. The total RNA was extracted and
21 subjected to Northern blot analysis. (B) The activity of negative-strand RNA3 synthesis
22 shown by the relative RNA3(-)/RNA3(+) ratio of the tested RNA3 derivatives compared with
23 that of 3S. The levels were measured using the ImageJ program, and the mean value and the
24 standard deviation were calculated based on three independent experiments.

25

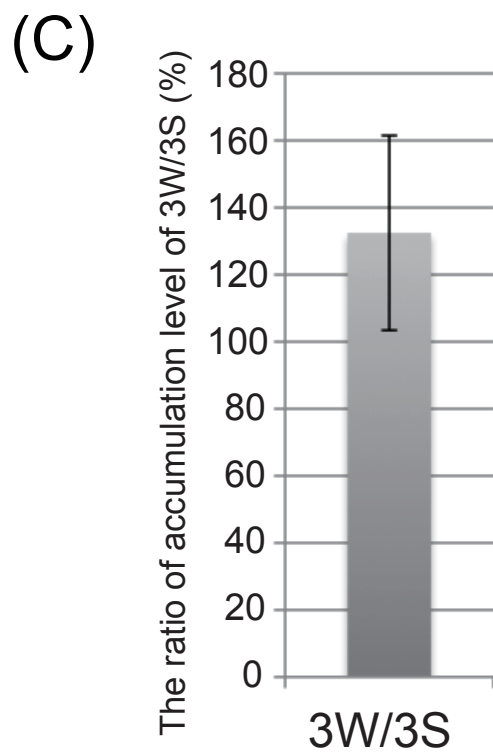
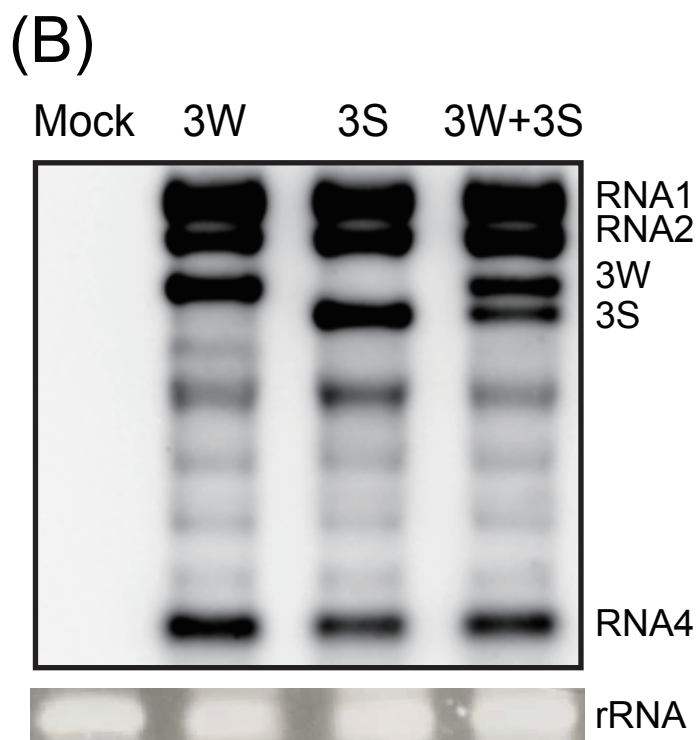
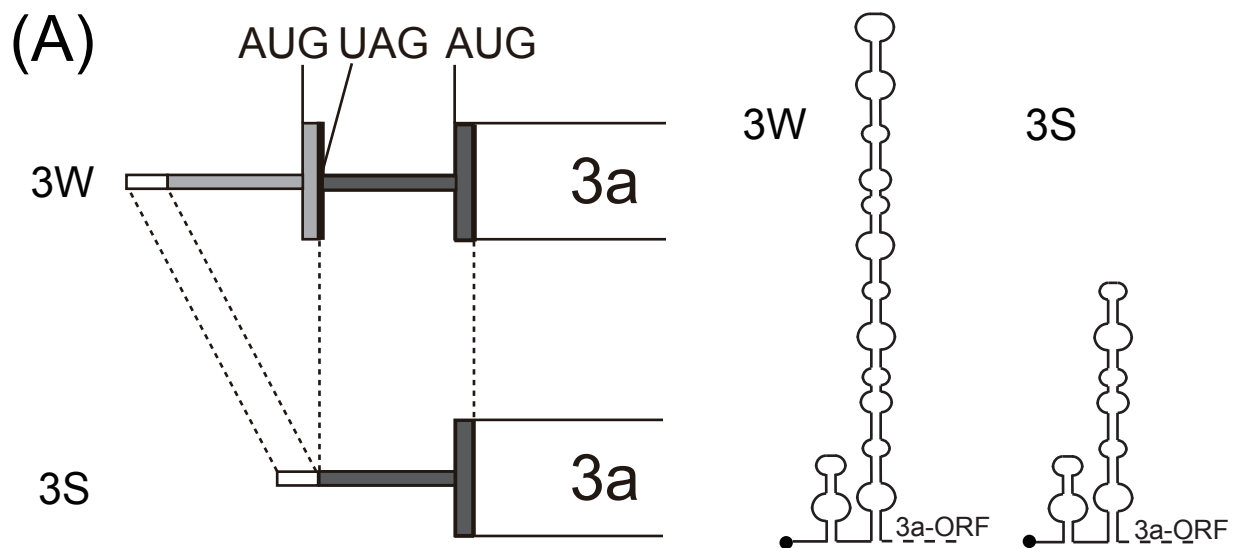
1 **Fig. 6.** Functional analysis of the similar base-paired structure of brome mosaic virus (BMV)
2 RNA3. (A) Predicted secondary RNA structures in the 5' UTR of RNA3 for six bromoviruses,
3 including base-paired regions (surrounded by dotted lines). The secondary RNA structures
4 were predicted using M-fold (Zuker, 2003). Accession numbers of the nucleotide sequences
5 of bromovirus RNA3s and ΔG (kcal/mole) values of the predicted structures of the 5' UTRs:
6 melandrium yellow fleck virus (MYFV, NC_013268; $\Delta G = -46.8$), BMV (NC_002028; $\Delta G =$
7 -20.3), cowpea chlorotic mottle virus (CCMV, NC_003542; $\Delta G = -56.6$), cassia yellow blotch
8 virus (CYBV, NC_007001; $\Delta G = -31.8$), spring beauty latent virus (SBLV, NC_004122; ΔG
9 $= -49.9$), and broad bean mottle virus (BBMV, NC_004006; $\Delta G = -69.3$). (B) Schematic
10 images of the base-paired regions of 3S and its derivatives. The deleted regions and a
11 four-nucleotide insertion are indicated by dotted lines and boldface italic letters, respectively.
12 (C) Northern blot analysis of viral RNA accumulation in *Nicotiana benthamiana* protoplasts
13 inoculated with 3S or its variants, together with MYFV RNA1 and RNA2 (MY1+MY2). The
14 numbers below the panel represent the accumulation levels of RNA3 relative to the internal
15 standard (coinoculated RNA1 and RNA2) and those of RNA4 relative to RNA3. The levels
16 were measured using the ImageJ program, and the mean values were calculated based on
17 three independent experiments. (D) Schematic images of the corresponding structures of
18 BMV RNA3 and its derivatives. The dotted lines indicate deleted regions. (E) Northern blot
19 analysis of viral RNA accumulation in *N. benthamiana* protoplasts inoculated with BMV
20 RNA3 or its variants, together with RNA1 and RNA2 of BMV (B1+B2) or the corresponding
21 MYFV RNAs (MY1+MY2). The levels were measured using the ImageJ program, and the
22 mean values were calculated based on three independent experiments.
23
24 **Supplementary Fig. S1.** Predicted structures of the 5' UTR of 3W and 3S. The secondary
25 RNA structures were predicted using M-fold (Zuker, 2003).

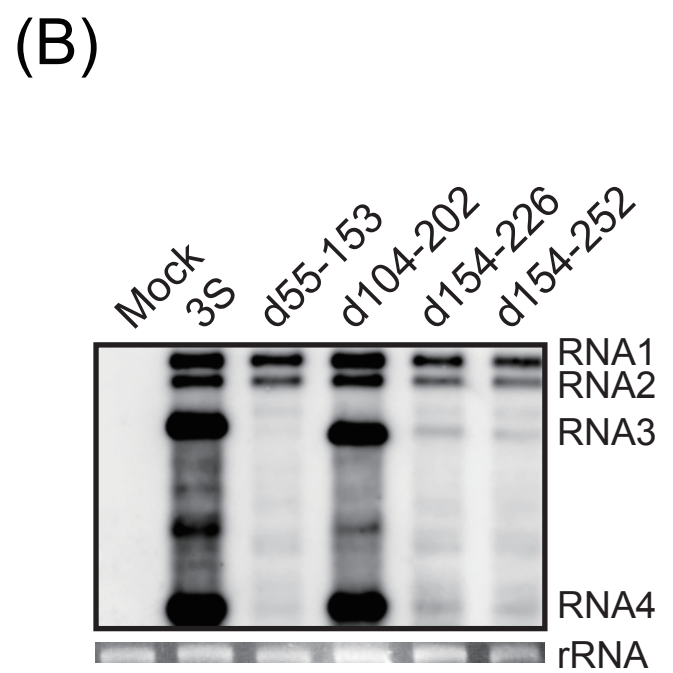
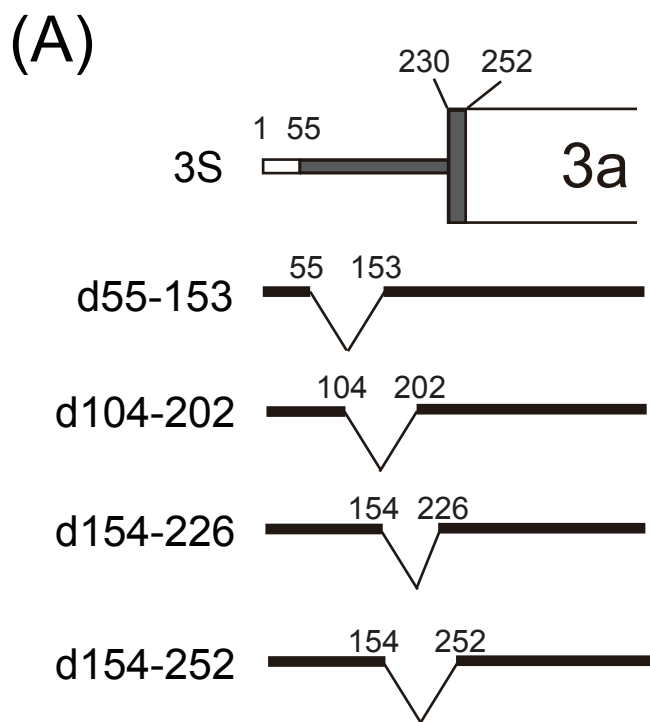
1
2 **Supplementary Fig. S2.** Temporal changes in the accumulation patterns of 3S and its
3 derivatives in two independent experiments (#1 and #2). RNAs were incubated in a cell-free
4 extract of evacuated BY-2 protoplasts (BYL). Total RNAs extracted from BYL at the
5 indicated times after incubation were subjected to Northern blot analysis using DIG-labeled
6 RNA probe specific to the 3'UTR of RNA3. Relative values for the accumulation of RNAs
7 were calculated and are shown between a pattern on a Northern blot and
8 ethidium-bromide-stained rRNA.

Supplementary Table S1

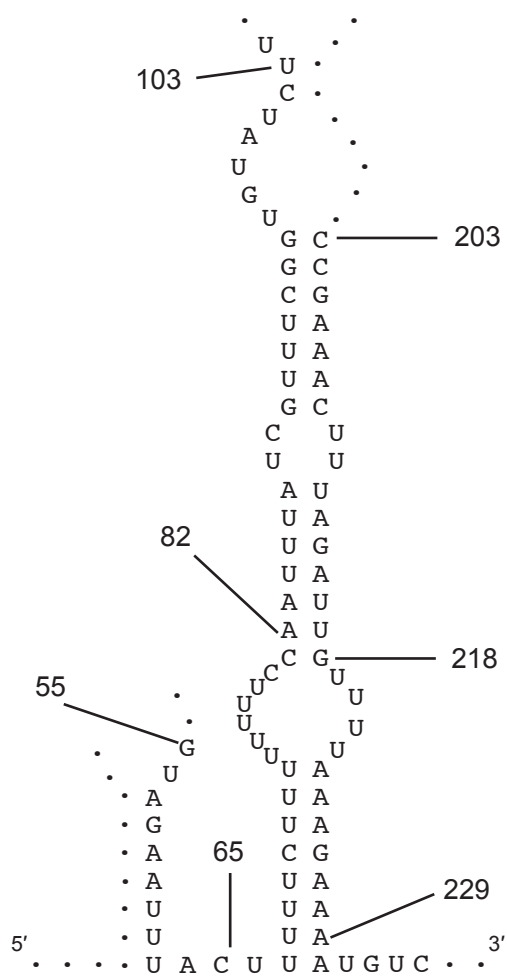
List of PCR primers and the nucleotide sequences used to generate constructs

Primer name	Sequence
M4	GTTTCCCAGTCACGAC
MY3.13R-2	GGTGC ACTCTTGATTATC
d55-153_F	CAACTAATTGGACGGCTTGAAGAAAATAC
d55-153_R	CCAAGCCGTCCAATTAGTTGCTTTATCGG
d104-202_F	CGGTGTATCTCCGAACTTTAGATTG
d104-202_R	CTAAAGTTTTCGGAGATACACCGAAACG
d154-226_F	GTCCTCCCGTTAAAATGTCTAACCTAGTTAAAC
d154-226_R	TTAGACATTTTAACGGGAGGACCTACTAAC
d154-252_F2	GGTCTCCCGTTATGACAGGTCGTTCTTC
d154-252_R2	CGACCTGTCATAACGGGAGGACCTACTAAC
d55-64_F	AAAGCAACTAATTCTTTTTCTTTTTTTCC
d55-64_R	AAAAGAAAAAGAATTAGTTGCTTTATCGG
d65-81_F	TTGTAGAATTTAAATTTATCGTTTCGGTG
d65-81_R	CGATAAATTTAAATTCTACAATTAGTTGC
d82-103_F	CTTTTTTTCTTAAAGGTTGGAACACACAG
d82-103_R	GTTCCAACCTTAAGGAAAAAAAAAGAAAAAG
d203-217_F	CCTCTCAGCGTTCGTTTTAAAGAAAATGTC
d203-217_R	CTTTAAAACGAACGCTGAGAGGAATTATAG
d218-229_F	AACTTTAGATTATGTCTAACCTAGTTAAAC
d218-229_R	CTAGGTTAGACATAATCTAAAGTTTCGGG
r1-1_F	GCGTTCGGCTTTGTTTAGATTGTTTTAAAG
r1-1_R	AACAAAGCCGAACGCTGAGAGGAATTATAG
r1-2_F	ATTTATCCAAAGCCTGTATCTTTAAGGTTG
r1-2_R	TACAGGCTTTGGATAAATTGGAAAAAAAAAG
r2-1_F	CCGAAACTTATTTAAGTTTTAAAGAAAATG
r2-1_R	CTTTAAA ACTTAAATAAGTTTCGGGAACGC
r2-2_F	TCCTTAGATTTCGTTTCGGTGTATCTTTAAG
r2-2_R	GAAACGAATCTAAGGAAAAAAAAAGAAAAAG
dMB-1_1	ATTGTAGAATTTACGGTGTATCTTTAAGG
dMB-1_2	TTAAAGATACACCGTAAATTCTACAATTAG
dMB-1_3	CAGCGTTCGGATGTCTAACCTAGTTAAAC
dMB-1_4	TTAACTAGGTTAGACATCGGGAACGCTGAG
dMB-2_1	TGTAGAATTTAACATCGGTGTATCTTTAAG
dMB-2_2	TACACCGATGTAAATTCTACAATTAGTTG
dMB3_F	AGTAGTGATACTGTTTTGTTCCCGATGTCTAACCTAGTTAAAC
dMB3_R	CAAAAACAGTATCACTACTGAAAAACCGATGTTAAATTCTAC
pBYL-MY1a_F	ATAAGAATGGCGCGCCATGGATCTATTAATTTAATTG
pBYL-MY1a_R	ATAAGAATGGCGCGCCTCAACTTACGCAAGCATC
pBYL-MY2a_F	ATAAGAATGGCGCGCCATGGCTTTCGAAATTGAATATG
pBYL-MY2a_R	ATAAGAATGGCGCGCCTTACTTAGAAAAAGAAGAC
Bd1_F	TAGTGATACTATGTCTAACATAGTTTCTCC
Bd1_R	TTAGACATAGTATCACTACTGAAAAACCG
Bd2_F	CTATTTTACCAATGTCTAACATAGTTTCTC
Bd2_R	GTTAGACATTGGTAAAATAGAATGTTTCGCC

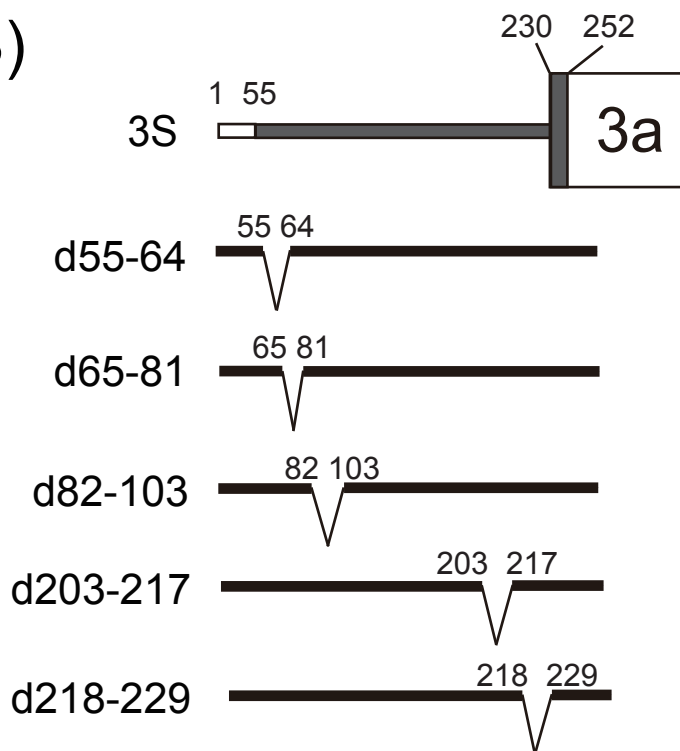




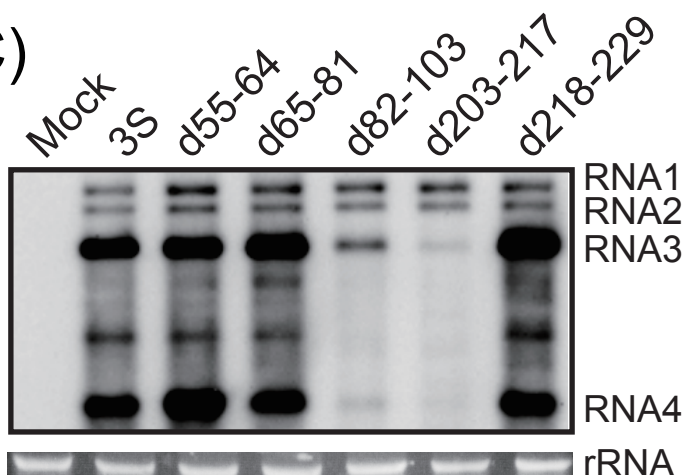
(A)



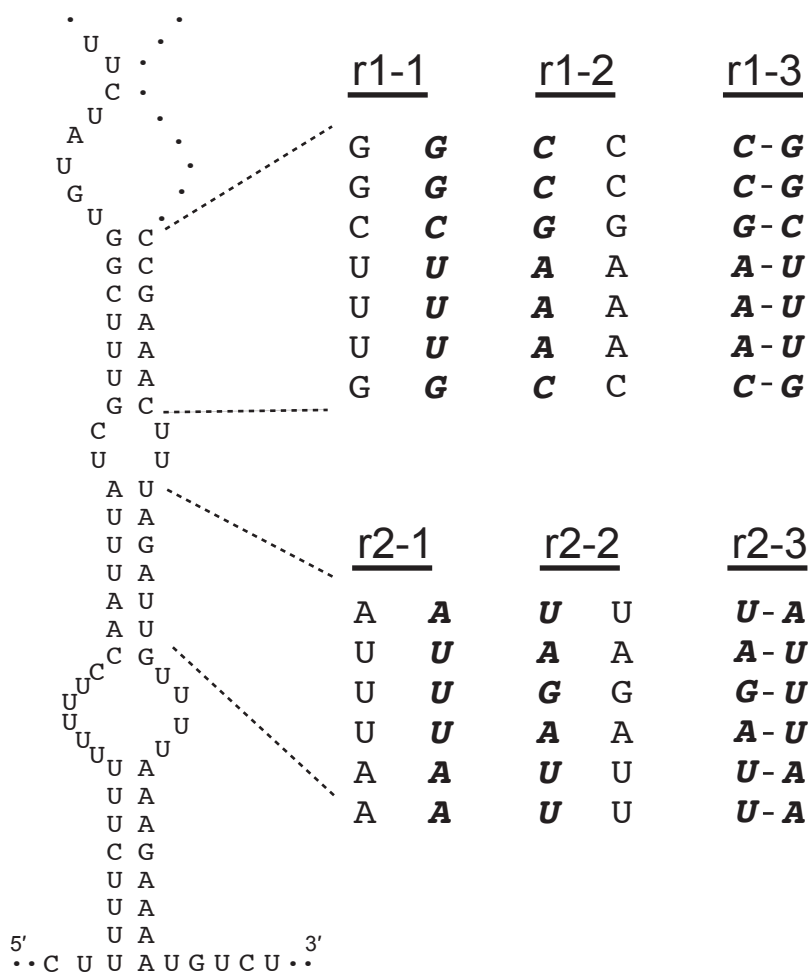
(B)



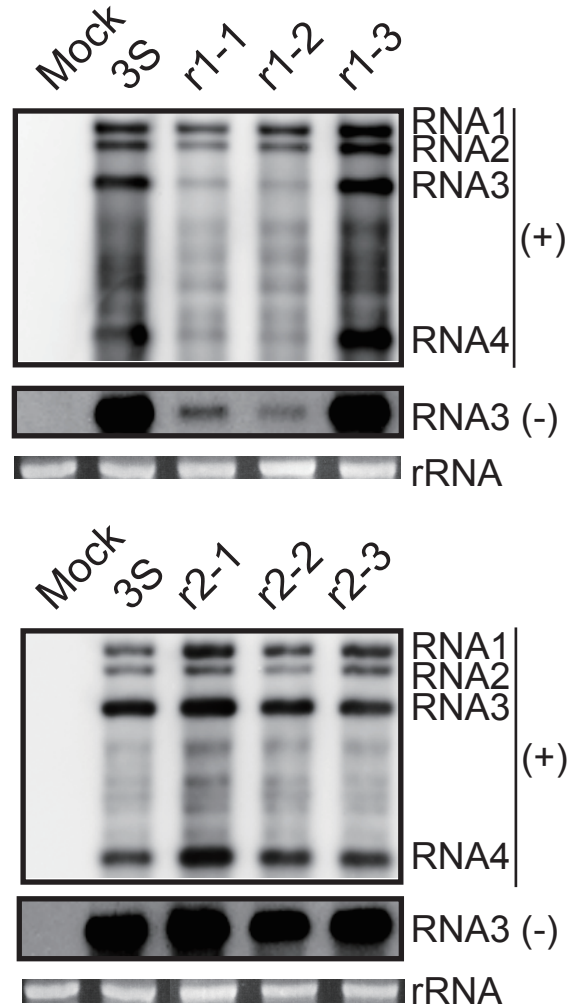
(C)



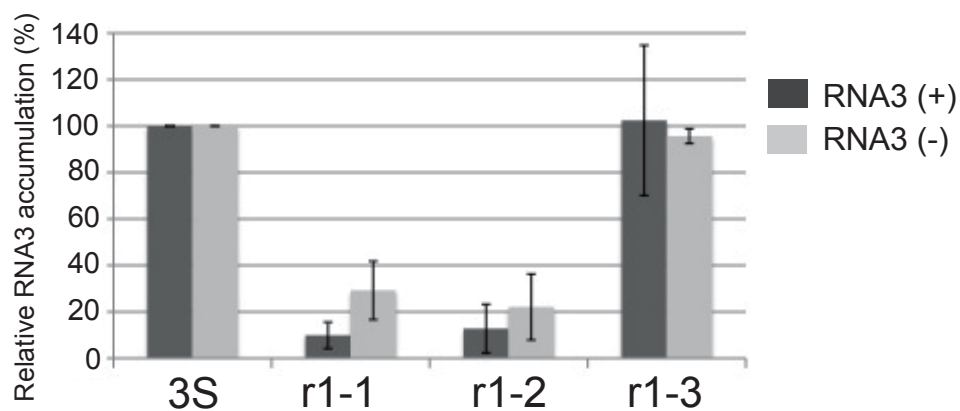
(A)

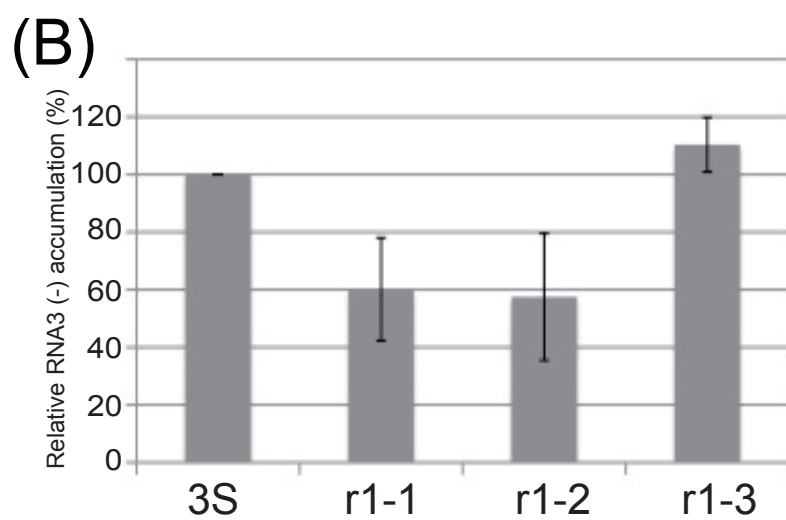
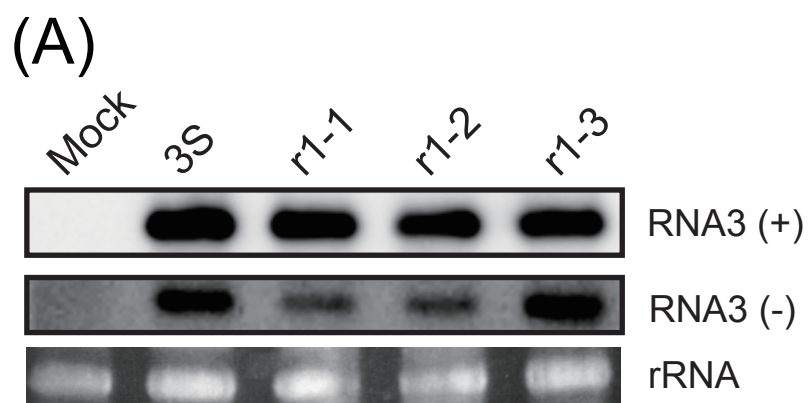


(B)

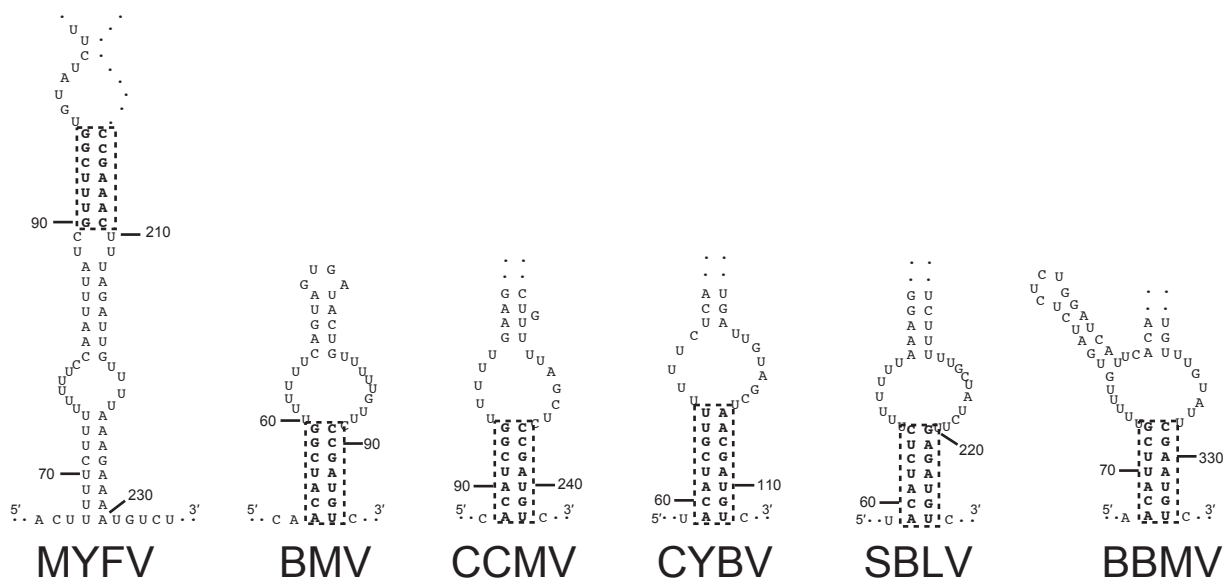


(C)

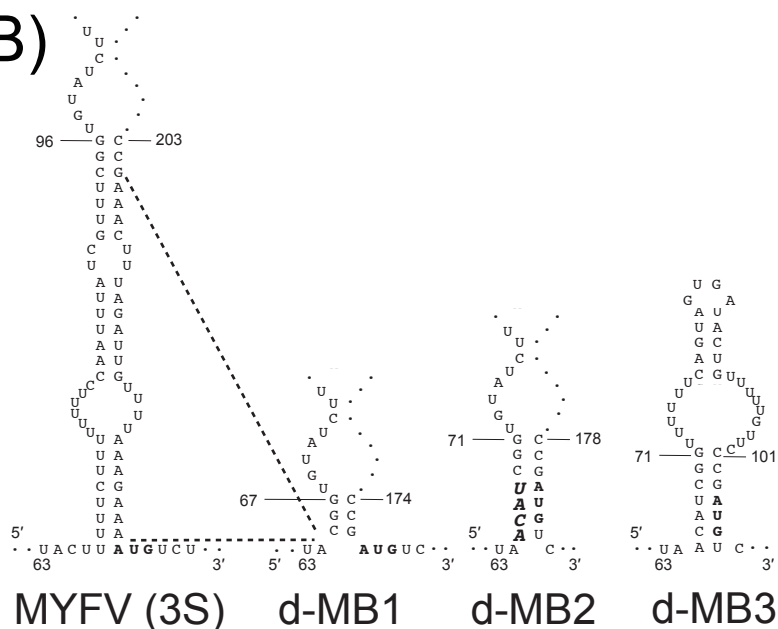




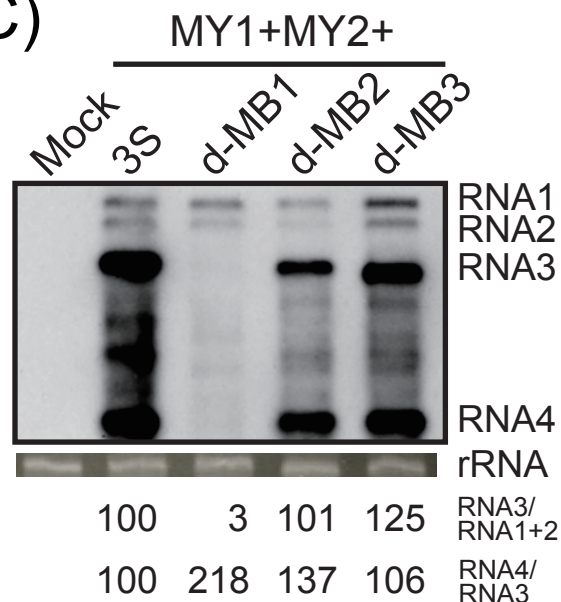
(A)



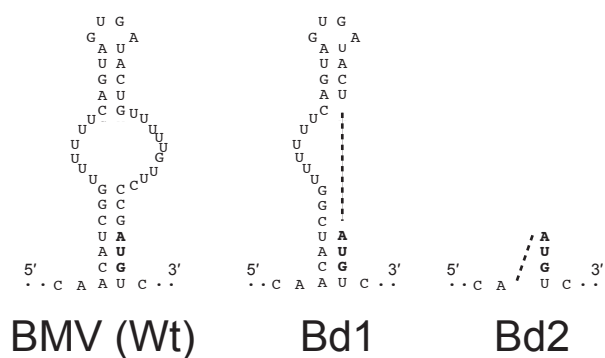
(B)



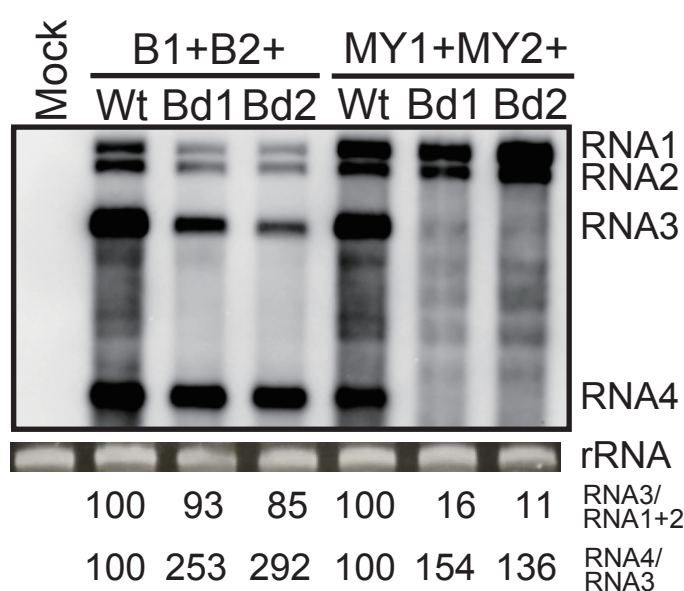
(C)

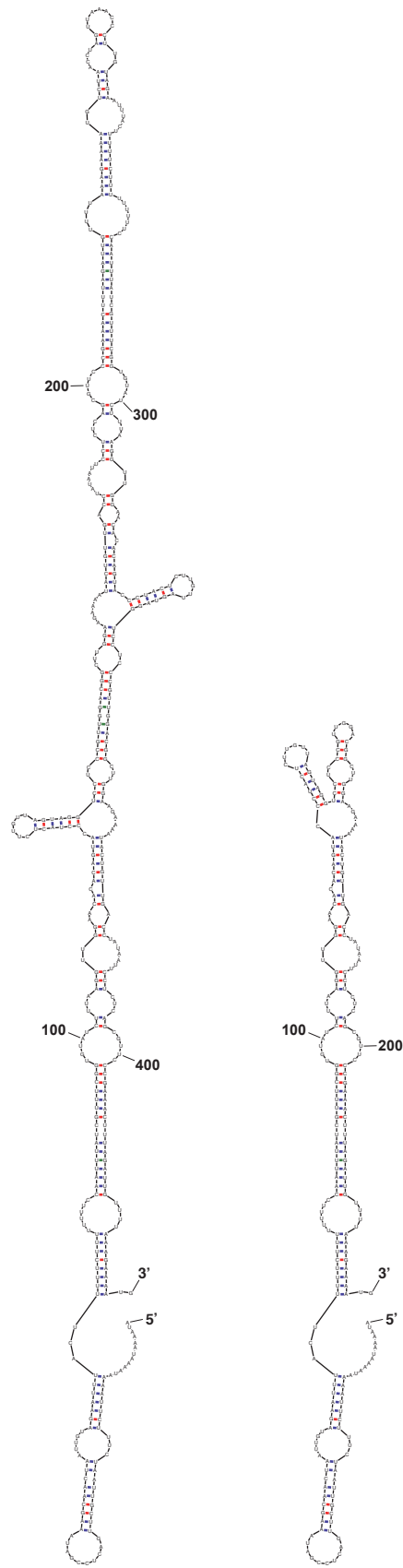


(D)



(E)





3W

3S

